

THE USE OF HYPERSPECTRAL DATA FOR EVALUATION OF WATER QUALITY PARAMETERS IN THE RIVER SAVA

Mak Kisevic^{1,*}, Mira Morovic², Roko Andricevic¹

¹Faculty of Civil Engineering, Architecture and Geodesy, University of Split, Split, Croatia

²Institute of Oceanography and Fisheries, Split, Croatia

ABSTRACT

The water quality monitoring through in situ sampling is costly and time consuming process that results in sparse point data difficult to achieve continuous water quality maps. Recent developments in remote sensing technology, especially in optical remote sensing, provide a significant potential to complement and enhance classical laboratory measurements. In this study we have assessed single band, first derivative and band ratio models for retrieving concentrations of chlorophyll *a*, turbidity and total suspended solids (TSS) from hyperspectral reflectance data collected along the River Sava. The spectral band ratio model showed the best correlation with Chl-*a* (R745/R418, $R^2 = 0.72$) and TSS (R373/R396, $R^2 = 0.78$), while the first derivative model had the best correlation with turbidity values ($R^2 = 0.87$). These results represent a promising first step in the initiative to develop a methodology for the water quality monitoring of the River Sava using remotely sensed data originating from various airborne and satellite hyperspectral sensors.

KEYWORDS:

hyperspectral; remote sensing; surface waters; water quality; eutrophication

INTRODUCTION

Escalating human population growth and industry pressures lead to nutrient over-enrichment and increase in eutrophication [1], which is a serious ecological problem causing a major concern in many coastal and inland water ecosystems [2,3]. Eutrophication of inland waters presents a persistent water quality problem through the overgrowth of algae and may affect not only the source of drinking water but also can be accumulated in the aquatic foods causing direct influence on the human health.

One of the major challenges for the environmental managers and decision makers is establishment of economic and reliable monitoring

system at watershed extent that would provide water quality data with sufficient spatial and temporal resolution. Such system would enable the assessment of land-based pollution sources as well as effectiveness of the wastewater treatment infrastructure or other management plans.

Varieties of satellite and air-borne remote sensing tools are being currently used for monitoring water quality parameters of surface waters. These water quality parameters can be quantified using remote sensing techniques allowing management plans to be formulated to reduce movement of substances from watersheds to water bodies, thus reducing the effects of the pollutants on water quality.

The optical remote sensing of rivers at the watershed scale is characterized by rapid results, low cost and provides important means to estimate chlorophyll *a* (Chl-*a*), total suspended solids (TSS) and turbidity values concentrations in surface waters. These parameters are often used to characterize general water quality and as an indicator of trophic state [4,5].

The Sava River flows through Slovenia, Croatia, along the northern border of Bosnia and Herzegovina, and through Serbia. This Southeast Europe River is a major contributor to the Danube watershed discharging in Belgrade. Its central part is a natural border of Bosnia and Herzegovina and Croatia. In addition to drinking water, sanitation and general household uses, the River Sava is also extensively used for river transport, agricultural and industrial production, as well as recreational purposes. Sava river is a low-productive water ecosystem. With the population growth and development the natural biological balance of Sava River has been disturbed by the increase of discharges from municipal and industrial wastewater pollution, as well as from agricultural runoff [6]. With the exception of the city of Zagreb municipal wastewaters are released in the River Sava in Croatia without any treatment or after primary treatment. There are however on-going projects for developing wastewater treatment capacity in the bigger towns.

The goal of the present study is to assess different models for the prediction of

concentrations of water quality parameters from the hyperspectral data and test the need for the implementation and development of specific local algorithms. In this study we also present the results of coupling water quality parameters and in-situ radiometric measurements. This is a first step in the initiative to develop a methodology for the water quality monitoring of the Sava River by using remotely sensed data originating from airborne and spaceborne multispectral and hyperspectral sensors.

MATERIALS AND METHODS

Data collection. Field data were acquired during the three-day data collection campaign in July 2010, which covered the whole stretch of the River Sava in Croatia (

FIGURE 1). We have chosen the locations upstream and downstream of bigger towns, including the city of Zagreb, to be able to estimate pollution contribution of the urban areas. The stations in the East are located in the most productive agricultural area in Croatia that represents the biggest non-point source pollution of the River Sava. In general point and non-point source pollution build up downstream from the border from Slovenia to the border with Serbia.

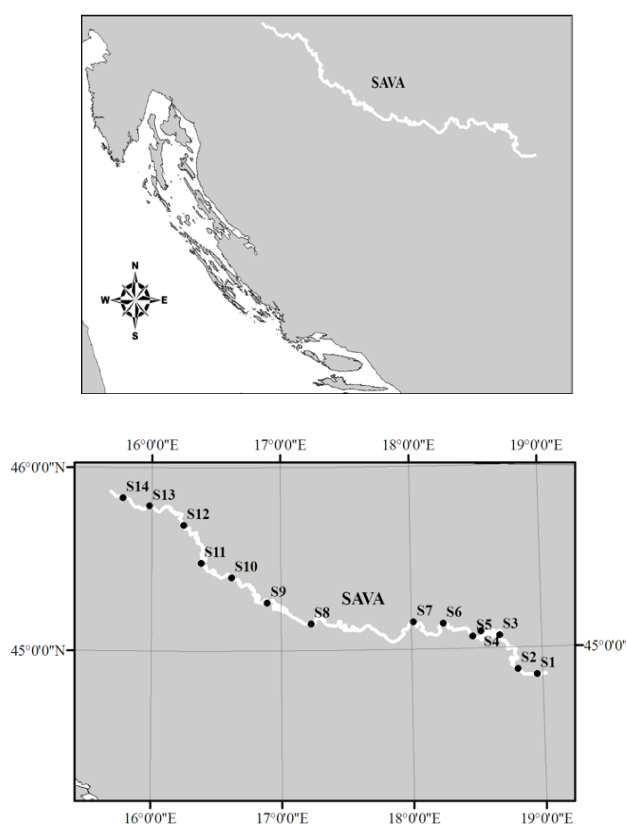


FIGURE 1
Measuring stations

The collected data consisted of laboratory measurements of in-situ water quality, spectral reflectance measurements above water surface and spectral reflectance measurements inside water column

Data were acquired on 14 monitoring stations under clear-weather conditions using two different measurement systems: above water and in-water spectroradiometers. Parallel to the radiometric data acquisition, the water samples were collected at 0.3 m below surface for laboratory analysis. These samples were stored in a cooler with ice in the dark, and taken back to the laboratory for analysis within 8 hours.

Spectral surface reflectance measurements were taken with the ASD FieldSpec® 3 VNIR spectrometer (350-1050 nm) with the attached fibre cable 70-90 cm above the water surface. The instrument was positioned at an angle 90–135° with the plane of the incident radiation away from the sun.

Downwelling radiance measurements, L_d ($W m^{-2} sr^{-1}$) were collected at each sample site using a 99% Spectralon panel as an optical standard for calibrating upwelling radiance. A dark reference was collected with each measurement of L_d .

In-water spectral reflectance measurements were obtained from the profiling radiometer PRR-800 (Biospherical inc.). The split PRR-800 configuration separates the radiance L_u and radiance E_d heads (cosine collector) and orients the detector plates in a horizontal plane. The profiler was lowered manually, from the sunny side of the standing platform until the bottom was reached. The data were processed with the use of Biospherical profiler software to produce surface water reflectance in all available 14 spectral bands: 340; 380; 412; 443; 465; 490; 510; 532; 555; 589; 625; 665; 683 and 710 nm.

Data preparation and statistical analysis. To eliminate the sun glint spectra and optimize the signal-to-noise ratio for in situ above water spectroradiometric data, the inconsistent radiance measurements were removed and the measurements at each site were averaged over at least 10 measurements. Such averaged measurements were transferred in tabular form used further in statistical analysis. The spectral range was trimmed from 1050 nm to 950 nm because of high water absorption of the signal in that NIR region. Statistical analysis was done using a statistical package R.

The evaluation between estimated water quality values (X_{est}) using spectral indices and analytically measured values (X_{meas}) is based on percentage difference:

$$e_j = 100 \cdot (X_{est_j} - X_{meas_j}) / X_{meas_j} \quad (1)$$

Mean normalized bias (MNB) is a measure of the over or under estimation of the observed values (systematic error). Those errors can in principle, be removed when the nature of the bias is identified. They are usually linked to the limitations of the measurement equipment or improper calibration.

The normalized root mean square error (NRMS) provides a good measure of data scatter for normally distributed variables (random error) and gives useful information of the accuracy between the estimated and observed data [7,8].

In this study we define MNB as follows:

$$MNB = \frac{1}{N} \sum_{i=1}^N e_i \quad (2)$$

while NRMS is represented with standard deviation of e

$$NRMS = \sqrt{\frac{1}{N} \sum_{i=1}^N (e_i - \bar{e})^2} \quad (3)$$

where N is the total number of samples and \bar{e} is mean value of e .

These measures of difference are often reported in similar studies to compare performance of different models.

RESULTS

Water quality data. The collected water samples were analysed in the laboratory for a number of water quality parameters. Analytically measured in-situ concentrations of optically visible water quality parameters are shown in TABLE 1. The difference between the minimum and maximum values is about one order of magnitude for all the examined parameters. The contrast between low values of Chl-a that are indicative to the oligotrophic waters and relatively high turbidity and TSS values was observed on most of the stations. One of the reasons is probably a rainy period that preceded the monitoring campaign and that caused high sediment levels in water runoff. Weak relationships between Chl-a ($r=0.1$)

concentrations and TSS values suggest higher amounts of non-algal turbidity in the water column in Sava River. Turbidity and TSS show strong positive relationship ($r=0.62$).

Spectral reflectance measurements. FIGURE 2 presents the above water reflectance values over various measuring stations. The general observed characteristics of the reflectance curves are shifting reflectance peak in the green-yellow region (560 nm), absorption peak at 670 nm and reflectance peak in near infrared (810 nm). NIR reflection peak at around 700 nm and absorption peak at 670 nm are not pronounced on all the spectral curves presumably because of the masking effect of suspended matter. TSS and turbidity increase the values of reflectance in the visible and NIR part of the spectrum [9].

Water surface condition characterized with waves and sun glint can have serious impact on the above water collection of spectral data [10]. The concurrent data acquired with these two instruments were used in order to verify the consistency of in-water and above-water measurements within our dataset and to examine the impact of surface conditions.

FIGURE 3 shows the difference between band ratios as measured by ASD FieldSpec and PRR-800 instrument just below the water surface in the space-time co-located stations. The two instruments show a fairly good agreement between ratios in green and blue spectral region ($MNB < 15.5\%$ and $NRMS < 1.3\%$) and larger bias in red and green ratio ($MNB = 33\%$ and $NRMS = 3\%$). This result is in line with the study from Bhatti et al. (2010) where they found that difference between above water and in-water spectral reflectance measurements was almost constant in blue and green region and minimal, but not consistent in the red region.

Correlation of spectral data and water quality parameters. In order to identify the most appropriate spectral regions for developing water quality retrieval algorithms, the relationship was examined between spectral data and analytically measured in-situ water quality parameters.

Raw spectral data were recalculated to single-band reflectance, first derivative of reflectance and reflectance ratios.

TABLE 1
The range of concentrations for Chl a, TSS and turbidity at the Sava River stations during the campaign in 2010

		N	Mean	SD	Min	Max
Chl a	[mg m ⁻³]	14	0.55	0.5	0.12	1.83
TSS	[mg l ⁻¹]	14	229.71	128.04	25.00	385.00
Turbidity	[NTU]	14	12.97	8.99	3.31	37.23

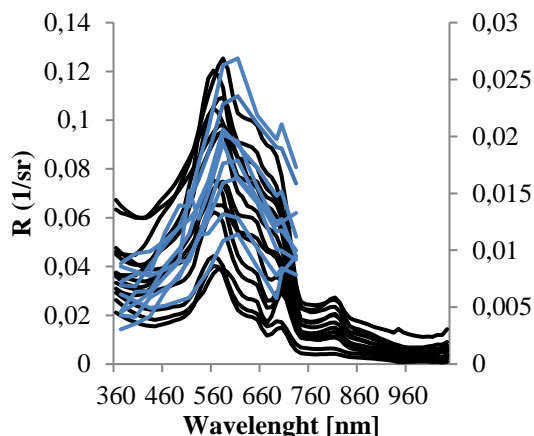


FIGURE 2
Reflectance values at different stations along the Sava River (black lines are spectra collected with ASD FieldSpec® and drawn on the left ordinate, blue lines are spectra collected with PRR-800 and drawn on the right ordinate)

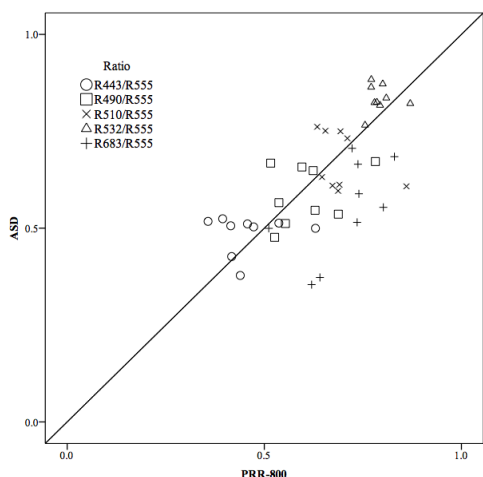
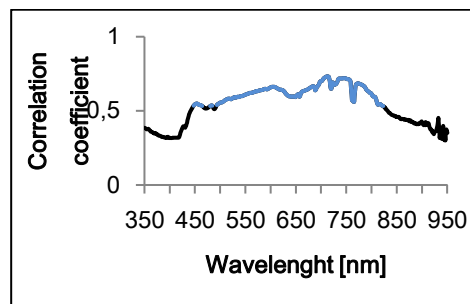


FIGURE 3
Comparison of ASD FieldSpec® and PRR-800 concurrent reflectance ratios

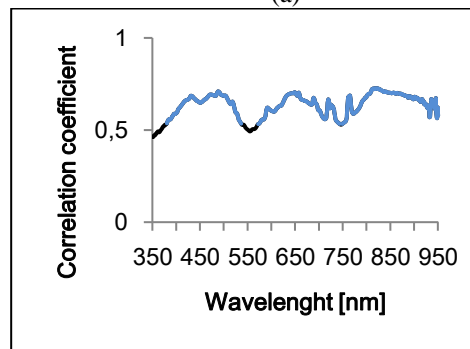
Single band reflectance. All 601 bands reflectance from 350 nm to 950 nm were correlated to Chl-a, TSS and turbidity values. The correlation curves showing Pearson correlation coefficient (r) are shown in **FIGURE 4**. It can be clearly observed that correlations are positive for all analysed water quality parameters. Single bands showing the strongest correlation with Chl-a, TSS and turbidity are presented in **TABLE 2**.

It can be observed that bands reflectance at wavelengths located in the local absorption peak and reflectance peak of the NIR region correlate strongest with Chl-a. This correlation in NIR region around 700 nm is well described in literature and

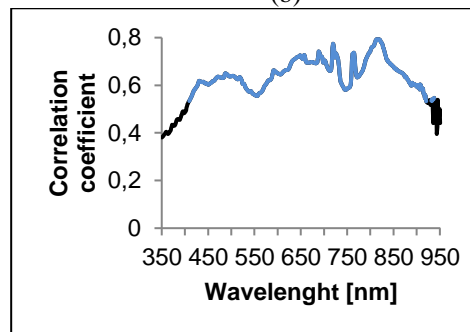
has been used for the estimation of chlorophyll concentrations [11-13].



(a)



(b)



(c)

FIGURE 4
Correlation coefficients between reflectance values and (a) Chl-a, (b) TSS and (c) Turbidity values; blue lines represent regions with statistical significance $p < 0.05$

TABLE 2
Spectral reflectance regions with the highest correlation coefficient (r) with Chl-a, TSS and turbidity.

	Chl-a		TSS		Turbidity	
Range [nm]	713	745	489	819	719	813
r	0.73	0.72	0.71	0.73	0.77	0.79

Correlation with TSS is strongest in the absorption peak of the blue-green region and reflectance peaks in NIR region. Turbidity is strongest correlated with the band in the reflectance peak in NIR region of the reflectance curve. Other

authors reported high correlation of single band reflectance with TSS in the region near 700 nm [13] and turbidity in the region near 710 nm [9] 570 nm [14].

First-derivative of reflectance. Derivative spectra indicate the rate of change of reflectance with wavelength giving us information on the slope of the reflectance curve at the certain wavelength. It is a useful tool for enhancing the spectral features that can be related to absorption bands of different optically visible water constituents [15].

Derivatives are often used to remove the background signal [16] and separate out peaks of overlapping bands [17]. They are also used as a method of data normalization since they are relatively less sensitive to the spectral variations of sunlight and skylight [18].

The strongest correlation with Chl-a (**FIGURE 5**) are found with the bands at 563 nm ($r = 0.80$), 750 nm ($r = 0.80$) and 753 nm ($r = 0.81$), which correspond to the reflectance peak in the green-yellow region and absorption peaks in the NIR region of the reflectance curve respectively. Han et al. (1997) [19] reports the best correlation in inland waters with the first derivative of reflectance at 690 nm and in coastal waters [20] with the first derivative of reflectance in the regions of 630–645 nm, 660–670 nm, 680–687 nm and 700–735 nm.

TSS has the highest correlation coefficient with the bands at 702 nm ($r = 0.81$), 706 nm ($r = 0.80$) and 804 nm ($r = 0.87$). These two regions are local reflectance peaks in NIR. The strongest correlation with turbidity is observed with the bands at 730 nm ($r = 0.91$), 821 nm ($r = 0.93$) and 826 nm ($r = 0.92$), which are, located in the local absorbance peaks of the NIR region.

Reflectance ratios. Reflectance ratios are widely used in the water quality retrieval algorithms, but they are not universally applicable [21]. Most of the algorithms developed for the retrieval of Chl-a concentrations are based on the peak near 700 nm [11] and the widely used NIR-red band ratio of R_{705}/R_{670} [9,12,22]. In recent studies some authors found other ratios to be more useful for Chl-a estimation from their datasets. Huang, Jiang et al. [21], found the highest correlation with the band ratio R_{861}/R_{866} ($r = 0.93$) Jiao, Zha et al. [23] report that the highest correspondence was achieved using the ratio of R_{719}/R_{667} ($r = 0.93$).

The band ratio of R_{705}/R_{670} showed no correlation in our data set. All the NIR-red band ratio combinations from R_{660} to R_{730} showed poor correlation. Furthermore, the band ratio R_{861}/R_{866} used by Huang (2010) showed also poor correlation with Chl-a values.

To find the reflectance band ratios that in our dataset correlate strongest with the water quality

parameters, a matrix with all possible spectral band ratios was created containing 180 000 combinations.

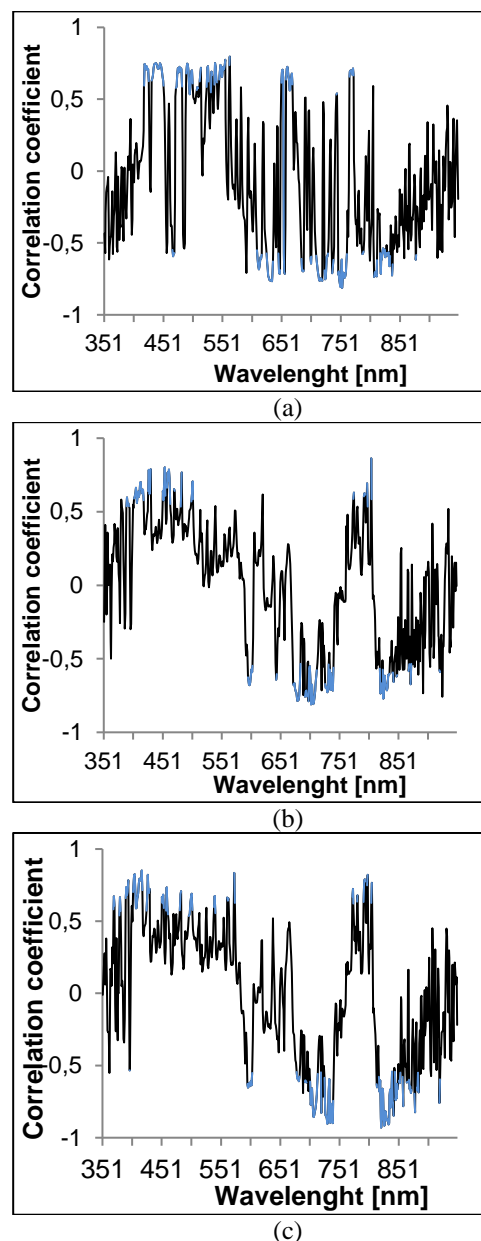


FIGURE 5
Correlation coefficients between first derivative of reflectance values and (a) Chl-a, (b) TSS and (c) Turbidity values; blue lines represent regions with statistical significance $p < 0.05$

To identify possible zones of interest, the obtained correlations were presented on the “heat maps” (FIGURE 6) where the location of each point corresponds to the ratio of wavelengths on the x and y axis and the point colour shows the absolute value of the correlation coefficient with the observed water quality parameter.

Band ratios R745/R418, R373/R396 and R396/R390 showed highest coefficients of determination respectively with Chl-a ($r = 0.85$), TSS ($r = 0.88$) and turbidity ($r = 0.85$).

For the Chl-a estimation it was expected to have one band in the NIR region, but it was unusual to find that the best correlation was between the ratio of NIR and violet/blue bands. To the best of our knowledge it is because of the optical properties of other water constituents mask phytoplankton pigment signals in blue-green region in turbid waters. These are typically dissolved colour substances like yellow substance, coloured mineral particles and eventually degraded plankton products.

Regression models. Linear regression models for the retrieval of the observed water quality parameters were developed with the spectral indices obtained using different presented methods (TABLE 3.).

The best of the observed models for Chl-a retrieval was bend ratio model showing MNB of 43.35% and NRMS of 25.94% with the highest

coefficient of determination ($R^2 = 0.72$). The first derivative model had MNB of 51.35% and NRMS of 28.34%. The most biased was a single band model with MNB of 58.47% and MRMS of 33.19%. All the observed models overestimated Chl-a values.

The same is observed for the estimation of TSS, where the band ratio model had the highest coefficient of determination ($R^2 = 0.78$), MNB of 15.91% and NMRS of 58.34%. The first derivative model was slightly worse with MNB of 19.65% and NMRS of 62.36%. The worst was again the single band model with MNB of 47.72% and NRMS of 84.77%

The single band model was the most precise for the estimation of turbidity with MNB of 6.59% and NMRS of 5.28%, but the lowest coefficient of determination ($R^2 = 0.63$). The first derivative model had MNB of 4.48% and MRMS of 24.95% with the highest coefficient of determination ($R^2 = 0.87$) and the band ratio model had lower coefficient of determination ($R^2 = 0.72$) with MNB of 9.25% and NMRS of 4.50%.

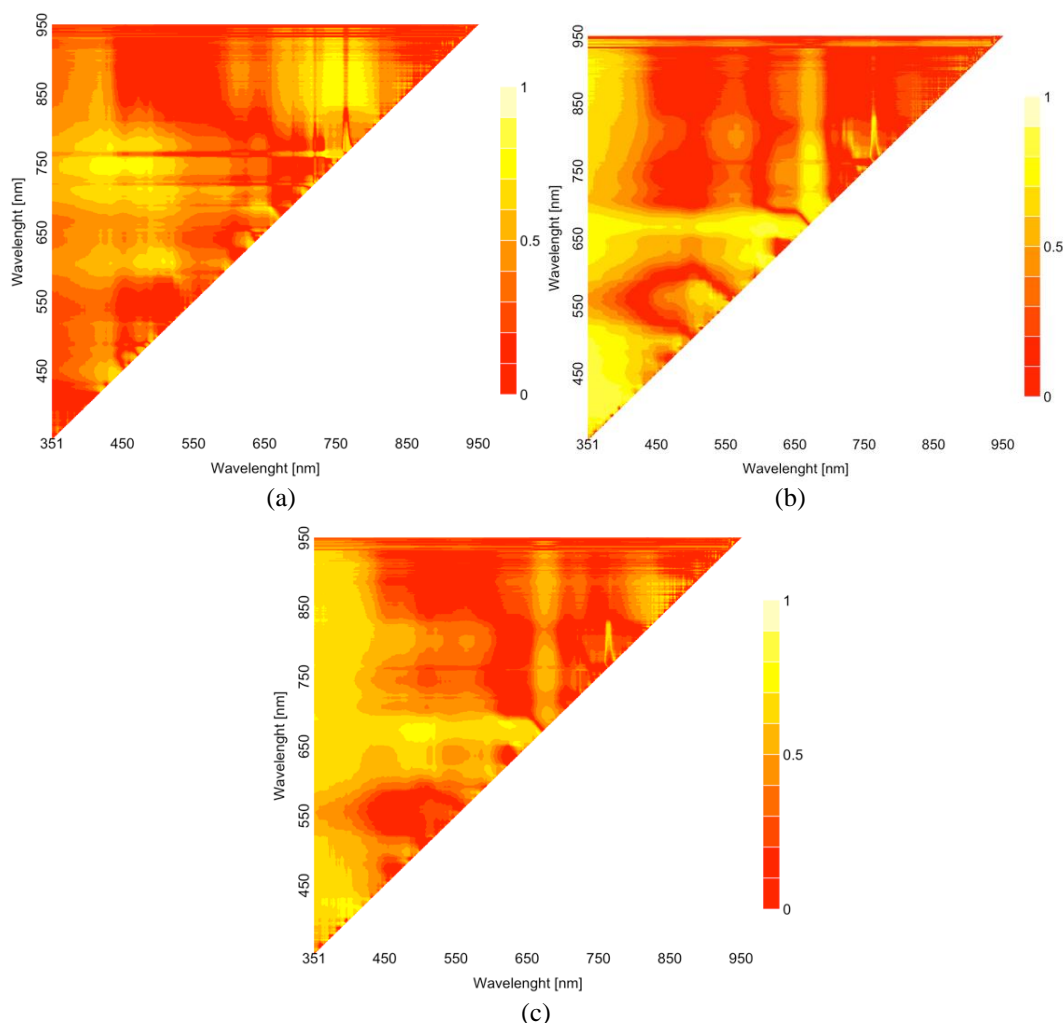


FIGURE 6

Correlation matrix between reflectance band ratios with a – Chl-a, b – TSS and c – turbidity. Scales on the right represent absolute value of Pearson's coefficient.



TABLE 3
Assessment of different models for the prediction of Chl-a, TSS and Turbidity values.

Parameter	Model	Bands	Regression equation	R ²	MNB	NMRS
Chl-a	Single band	R713	17.71 x R713 - 0.13	0.54	58.47%	33.19%
Chl-a	First derivative	R753	-15077.19 x R753 + 0.02	0.66	51.35%	28.34%
Chl-a	Band ratio	R745/R418	3.31 x R745/R418 - 0.84	0.72	43.35%	25.94%
TSS	Single band	R813	13086.31 x R813 + 23.71	0.53	47.72%	84.77%
TSS	First derivative	R804	3589757 x R804 + 0.76	0.75	19.65%	62.36%
TSS	Band ratio	R373/R396	-2447.52 x R373/R396 + 2811.57	0.78	15.91%	58.34%
Turbidity	Single band	R819	957.58 x R813 - 2.91	0.63	6.59%	5.28%
Turbidity	First derivative	R821	-56956.11 x R821 - 0.42	0.87	4.48%	24.95%
Turbidity	Band ratio	R396/R390	537.51 x R396/R390 - 521.12	0.72	9.25%	4.50%

DISCUSSION AND CONCLUSIONS

In this study we discussed the potentials to use hyperspectral data to predict concentrations of water quality parameters in inland waters.

Presented were the results of coupling water quality parameters Chl-a, TSS and turbidity with field radiometric measurements taken along the Sava River.

All the developed algorithms overestimated water quality values. The best precision and accuracy were obtained for the algorithms for turbidity estimations.

NIR reflection peak at around 700 nm and absorption peak at 670 nm are not pronounced on all the reflectance spectra presumably because of the masking effect of high concentrations of suspended matter.

The best algorithm for Chl-a was based on the R745/R418 band ratio model showing high correlation with measured values ($R^2 = 0.72$) with MNB of 43.35% and NRMS of 25.94%. The well documented algorithm based on NIR/Red reflectance band ratio performed very poor in our study with $R^2 < 0.05$.

The best algorithm for TSS retrieval ($R^2 = 0.78$) was based on the R373/R396 band ratio model, but opposite to Chl-a algorithm, showing a high dissipation.

The first derivative model showed as a best predictor for turbidity values ($R^2 = 0.87$) MNB of 4.48% and MRMS of 24.95%.

The results of our study suggest that the band ratios used are useful to estimate water quality, but that the larger set of data is needed to achieve greater precision. The models developed will enable using data acquired from hyperspectral airborne and satellite sensors for monitoring water

quality. This will provide cost-effective method for mapping Chl-a, TSS or turbidity values and possibly using them as proxy for evaluating trophic state and nutrient enrichment of the River Sava and similar inland waters.

ACKNOWLEDGEMENTS

This work was partially funded by the Swedish Research Council (VR; project number 2009-3221).

We would like to specially thank professor Gia Destouni for continuous support and discussions regarding the use of hyperspectral data for complementing the monitoring of nutrient dynamics.

REFERENCES

- [1] Selman, M., Greenhalgh, S., Diaz, R. and Sugg, Z. (2008) Eutrophication and hypoxia in coastal areas: a global assessment of the state of knowledge. World Resources Institute. World Resource Institute, Washington.
- [2] Lotze, H.K., Lenihan, H.S., Bourque, B.J., Bradbury, R.H., Cooke, R.G., Kay, M.C. et al. (2006) Depletion, degradation, and recovery potential of estuaries and coastal seas. *Science*, American Association for the Advancement of Science. **312**, 1806–9.
- [3] Vitousek, P.M., Aber, J.D., Howarth, R.W., Likens, G.E., Matson, P.A., Schindler, D.W. et al. (1997) Human alteration of the global

- nitrogen cycle: sources and consequences. *Ecological Applications*, Eco Soc America. **7**, 737–50.
- [4] Vollenweider, R.A., Giovanardi, F., Montanari, G. and Rinaldi, A. (1998) Characterization of the trophic conditions of marine coastal waters, with special reference to the NW Adriatic Sea: proposal for a trophic scale, turbidity and generalized water quality index. *Environmetrics*, **9**, 329–57.
- [5] Mssanzya, S.M. (2010) Monitoring and Predicting Eutrophication of Inland Waters Using Remote Sensing. International Institute for Geo-information Science and Earth Observation, [Enschede]. pp. 1–63.
- [6] Ogrinc, N., Markovics, R., Kanduc, T. and Walter, L. (2008) Sources and transport of carbon and nitrogen in the River Sava watershed, a major tributary of the River Danube. *Applied Geochemistry*, 3685–98.
- [7] Gitelson, A., Dall'Olmo, G., Moses, W., Rundquist, D., Barrow, T., Fisher, T. et al. (2008) A simple semi-analytical model for remote estimation of chlorophyll-a in turbid waters: validation. *Remote Sensing of Environment*, **112**, 3582–93.
- [8] Ouillon, S. and Petrenko, A. (2005) Above-water measurements of reflectance and chlorophyll-a algorithms in the Gulf of Lions, NW Mediterranean Sea. *Optics Express*, **13**, 2531–48.
- [9] Kallio, K., Kutser, T., Hannonen, T., Koponen, S., Pulliainen, J., Vepsäläinen, J. et al. (2001) Retrieval of water quality from airborne imaging spectrometry of various lake types in different seasons. *The Science of the Total Environment*, **268**, 59–77.
- [10] Bhatti, A.M., Rundquist, D., Schalles, J., Steele, M. and Takagie, M. (2010) Qualitative assessment of inland and coastal waters by using remotely sensed data. In: Kajiwara K, Muramatsu K, Soyama N, Endo T, Ono A, Akatsuka S, editors. Kyoto.
- [11] Gitelson, A. (1992) The peak near 700 nm on radiance spectra of algae and water: relationships of its magnitude and position with chlorophyll concentration. *International Journal of Remote Sensing*, Taylor & Francis. **13**, 3367–73.
- [12] Dekker, A.G. (1993) Detection of Optical Water Quality Parameters for Eutrophic Waters by High Resolution Remote Sensing. Vrije Universiteit Amsterdam, [Amsterdam]. pp. 1–237.
- [13] Senay, G.B., Shafique, N.A., Autrey, B.C., Fulk, F. and Cormier, S.M. (2002) The selection of narrow wavebands for optimizing water quality monitoring on the Great Miami River, Ohio using hyperspectral remote sensor data. *Journal of Spatial Hydrology*, **1**, 1–22.
- [14] Chen, S., Fang, L., Zhang, L. and Huang, W. (2009) Remote sensing of turbidity in seawater intrusion reaches of Pearl River Estuary - A case study in Modaomen water way, China. *Estuarine Coastal and Shelf Science*, **82**, 119–27. <http://dx.doi.org/10.1016/j.ecss.2009.01.003>
- [15] Torrecilla, E., Píera, J. and Vilaseca, M. (2009) Derivative analysis of hyperspectral oceanographic data. *Advances in Geoscience and Remote Sensing*, INTECH Open Access Publisher. 597–618.
- [16] Becker, B.L., Lusch, D.P. and Qi, J. (2005) Identifying optimal spectral bands from in situ measurements of Great Lakes coastal wetlands using second-derivative analysis. *Remote Sensing of Environment*, Elsevier. **97**, 238–48.
- [17] Morrey, J.R. (1968) On determining spectral peak positions from composite spectra with a digital computer. *Analytical Chemistry*, ACS Publications. **40**, 905–14.
- [18] Tsai, F. and Philpot, W. (1998) Derivative analysis of hyperspectral data. *Remote Sensing of Environment*, Elsevier. **66**, 41–51.
- [19] Han, L. and Rundquist, D.C. (1997) Comparison of NIR/RED ratio and first derivative of reflectance in estimating algal-chlorophyll concentration: A case study in a turbid reservoir. *Remote Sensing of Environment*, Elsevier. **62**, 253–61.
- [20] Han, L. (2005) Estimating chlorophyll-a concentration using first-derivative spectra in coastal water. *International Journal of Remote Sensing*, **26**, 5235–44.
- [21] Huang, Y., Jiang, D., Zhuang, D. and Fu, J. (2010) Evaluation of Hyperspectral Indices for Chlorophyll-a Concentration Estimation in Tangxun Lake (Wuhan, China). *International Journal of Environmental Research and Public Health*.
- [22] Mittenzwey, K.H. (1992) Determination of chlorophyll a of inland waters on the basis of spectral reflectance. *Limnology and Oceanography*, American Society of Limnology and Oceanography. **37**, 147–9.



- [23] Jiao, H.B., Zha, Y., Gao, J., Li, Y.M., Wei, Y.C. and Huang, J.Z. (2006) Estimation of chlorophyll - a concentration in Lake Tai, China using in situ hyperspectral data. *International Journal of Remote Sensing*, Taylor & Francis. **27**, 4267–76.

Received: 29.02.2016

Accepted: 19.07.2016

CORRESPONDING AUTHOR

Mak Kisevic

Faculty of Civil Engineering,
Architecture and Geodesy,
University of Split, Matice hrvatske 15 ,
HR-21000 Split, Croatia

e-mail: kisevic@gmail.com